

Second-harmonic parametric scattering in ferroelectric crystals with disordered nonlinear domain structures

Jose Trull¹, Crina Cojocaru¹, Robert Fischer^{2,4}, Solomon M. Saitiel^{2,3},
Kestutis Staliunas¹, Ramon Herrero¹, Ramon Vilaseca¹,
Dragomir N. Neshev², Wieslaw Krolikowski⁴, and Yuri S. Kivshar²

¹*Departament de Física i Enginyeria Nuclear, Escola Tècnica Superior d'Enginyeries Industrial y Aeronàutica de Terrassa, Universitat Politècnica de Catalunya, Colom 11, Terrassa, 08222 Barcelona, Spain*
crina.maria.cojocaru@upc.edu

²*Nonlinear Physics Center and Australian Research Council Center for Ultra-high bandwidth Devices for Optical Systems (CUDOS), Australian National University, Canberra, ACT 0200, Australia*
dragomir.neshev@anu.edu.au

³*Faculty of Physics, University of Sofia, 5 J. Bourchier Boulevard, BG-1164 Sofia, Bulgaria*
saitiel@phys.uni-sofia.bg

⁴*Laser Physics Center and Australian Research Council Center for Ultra-high bandwidth Devices for Optical Systems (CUDOS), Australian National University, Canberra ACT 0200, Australia*
wzk111@rsphysse.anu.edu.au

Abstract: We study the second-harmonic (SH) parametric processes in unpoled crystals of Strontium Barium Niobate (SBN) with disordered structures of ferroelectric domains. Such crystals allow for the simultaneous phase matching of several second-order nonlinear processes. We analyze the polarization properties of these parametric processes using two types of generation schemes: quasi-collinear SH generation and transverse SH generation. From our experimental data we determine the ratio of d_{32} and d_{33} components of the second order susceptibility tensor and also the statistical properties of the random structure of the SBN crystal.

© 2007 Optical Society of America

OCIS codes: (190.0190) Nonlinear optics; (190.2620) Harmonic generation and mixing; (190.4420) Nonlinear optics, transverse effects; (190.4720) Optical nonlinearities of condensed matter; (290.0290) Scattering.

References and links

1. F. Zernike and J. E. Midwinter, *Applied Nonlinear Optics* (Wiley, New York, 1973).
2. M. M. Fejer, G. A. Magel, D. H. Jundt, and R. L. Byer, "Quasi-phase-matched second harmonic generation: tuning and tolerances," *IEEE J. Quantum Electron.* **QE-28**, 2631-2654 (1992).
3. M. Baudrier-Raybaut, R. Haidar, Ph. Kupecek, Ph. Lemasson, and E. Rosencher, "Random quasi-phase-matching in bulk polycrystalline isotropic nonlinear materials," *Nature (London)* **432**, 374-376 (2004).
4. S. E. Skipetrov, "Disorder is the new order," *Nature (London)* **432**, 285-286 (2004).
5. E. Yu. Morozov, A. A. Kaminskii, A. S. Chirkin, and D. B. Yusupov, "Second optical harmonic generation in nonlinear crystals with a disordered domain structure," *JETP Lett.* **73**, 647-650 (2001).
6. X. Vidal and J. Martorell, "Generation of light in media with a random distribution of nonlinear domains," *Phys. Rev. Lett.* **97**, 013902 (2006).
7. A. R. Tunyagi, M. Ulex, and K. Betzler, "Noncollinear optical frequency doubling in strontium barium niobate," *Phys. Rev. Lett.* **90**, 243901 (2003).

8. R. Fischer, D. N. Neshev, S. M. Saltiel, W. Krolikowski, and Yu. S. Kivshar, "Broadband femtosecond frequency doubling in random media," *Appl. Phys. Lett.* **89**, 191105(3) (2006).
9. R. Fischer, D. N. Neshev, S. M. Saltiel, A. A. Sukhorukov, W. Krolikowski, Yu. S. Kivshar, "Monitoring ultrashort pulses by transverse frequency doubling of counterpropagating pulses in random media," *Appl. Phys. Lett.* **91**, 031104(3) (2007).
10. B. F. Johnston, P. Dekker, M. J. Withford, S. M. Saltiel, and Yu. S. Kivshar, "Simultaneous phase matching and internal interference of two second-order nonlinear parametric processes," *Opt. Express* **14**, 11756-11765 (2006).
11. J. J. Romero, C. Arago, J. A. Gonzalo, D. Jaque, and J. Garcia Sole, "Spectral and thermal properties of quasi-phase-matching second-harmonic generation in $\text{Nd}^{3+}:\text{Sr}_{0.6}\text{Ba}_{0.4}(\text{NbO}_3)_2$ multi-self-frequency-converter nonlinear crystals," *J. Appl. Phys.* **93**, 3111-3113 (2003).
12. M. O. Ramirez, D. Jaque, L. Ivleva, and L. E. Bausa, "Evaluation of ytterbium doped strontium barium niobate as a potential tunable laser crystal in the visible," *J. Appl. Phys.* **95**, 6185-6191 (2004).
13. M. Horowitz, A. Bekker, and B. Fischer, "Broadband second-harmonic generation in $\text{SrBaNb}_2\text{O}_6$ by spread spectrum phase matching with controllable domain gratings," *Appl. Phys. Lett.* **62**, 2619-2621 (1993).
14. Th. Woike, T. Granzow, U. Dörfler, Ch. Poetsch, M. Wöhlecke, and R. Pankrath, "Refractive Indices of Congruently Melting $\text{Sr}_{0.61}\text{Ba}_{0.39}\text{Nb}_2\text{O}_6$," *Phys. Status Solidi A* **186**, R13-R15 (2001).
15. E. Yu. Morozov and A. S. Chirkin, "Stochastic quasi-phase matching in nonlinear-optical crystals with an irregular domain structure," *Sov. J. Quantum Electron.* **34**, 227-232 (2004).
16. Y. Le Grand, D. Rouede, C. Odin, R. Aubry, and S. Mattauch, "Second-harmonic scattering by domains in RbH_2PO_4 ferroelectric," *Opt. Commun.* **200**, 249-260 (2001).
17. G. Dolino, "Effects of domain shapes on second harmonic scattering in Triglycine Sulfate," *Phys. Rev. B* **6**, 4025-4035 (1972).
18. C. R. Jeggo and G. D. Boyd, "Nonlinear optical polarizability of the Niobium-Oxygen bond," *J. Appl. Phys.* **41**, 2741-2743 (1970).

1. Introduction

Nonlinear parametric processes in optics are known to depend critically on the phase matching between the parametrically interacting waves, most frequently achieved by utilizing the crystal birefringence [1] or by employing the so-called quasi-phase-matching (QPM) technique [2]. The phase matching requirements enable efficient nonlinear interactions but they limit the spectral bandwidth of the nonlinear optical process, making the designed frequency converter only suitable for a fixed input wavelength and single interaction. However, it has been shown recently that disordered nonlinear media allows the phase matching in a broad bandwidth regime of the frequency conversion [3, 4, 5, 6, 7]. An example of a quadratic nonlinear medium with a randomized domain structure is an unpoled Strontium Barium Niobate (SBN) crystal. Such crystals are composed of a system of random-size anti-parallel ferroelectric domains that allow to phase-match any second-order parametric process, including the second-harmonic generation (SHG) [7, 8], over a broad range of wavelengths without any poling. The bandwidth limitations are mainly given by the transparency window of the crystal in the range of 0.4-6 μm . Recently, we have shown that this ultra-broad parametric generation can be used to map complex infrared spectra into visible [8] or for short-pulse monitoring [9].

In this paper, we study experimentally and theoretically coherence and polarization properties of the second-harmonic (SH) waves generated in SBN crystals with disordered ferroelectric domains. By varying the input polarization, we demonstrate several simultaneous phase-matched SH processes which contribute to the total measured SH signal. We show that, unlike the perfect periodic structures where signals generated by different processes are coherent [10], the disordered medium leads to an incoherent superposition of different processes. Our experimental results and theoretical analysis allow to determine statistical parameters of such random nonlinear structures.

2. Experimental setups and results

We use two different setups for the experimental studies of parametric interactions. In the first case, we generate a quasi-collinear SH signal with either single fundamental beam or two fun-

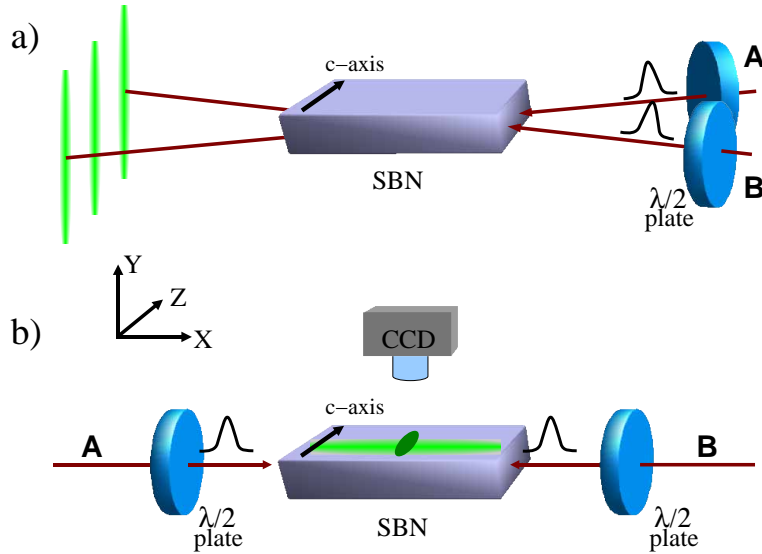


Fig. 1. Schematic representation of the two experiments: (a) QCSH experiment with the observation of a single SH beam and SH with small noncollinear angle of the fundamental beams; (b) TSH experiment with a single pulse and/or two counter-propagating pulses. In both cases the optical c-axis of the crystal is perpendicular to the plane of drawing.

fundamental beams propagating at a small relative angle. Below in the paper we refer to this setup as the QCSH experiment: **Q**uasi **C**ollinear **S**econd **H**armonic experiment. In the second case, the generated SH wave propagates transversely to the fundamental beam, and we refer to this setup as the TSH experiment: **T**ransverse **S**econd **H**armonic experiment.

The QCSH experiment is based on a nanosecond Nd:YAG system operating at 1064 nm. The nanosecond system (pulse duration $\tau = 8$ ns, repetition rate 10 Hz) is arranged to deliver two beams (which we refer to as beams **A** and **B**) with total energy of 3 mJ each and diameter of 5 mm (FWHM). The beams intersect at the external angle 4° inside an unpoled SBN crystal.

The TSH experiment employs the femtosecond MIRA generator with tuning capability in the range of 800 – 900 nm. The femtosecond setup (pulse duration $\tau = 150$ fs, repetition rate 76 MHz) is arranged to deliver two counter-propagating beams with power 300 mW and diameter 1 mm. The two beams are loosely focused in the crystal. The beam paths are chosen in such a way that the counter-propagating pulses meet in the central part of the SBN crystal. The use of femtosecond pulses is essential for this geometry as the pulse length is shorter than the crystal length, allowing to distinguish between the single beam contribution to the SH signal and SH due to **A** and **B** mixing.

In both experimental setups the polarization orientation of the entering beams **A** and **B** is controlled by $\lambda/2$ wave plates. The geometries of the two experimental setups are shown schematically in Figs. 1(a,b), respectively.

Two samples of an unpoled SBN crystal with the dimensions 5x5x20 mm and 5x5x10 mm have been used in the QCSH and TSH experiments, respectively. The 4mm point symmetry group of the SBN crystal determines the nonzero components of the second-order susceptibility tensor, $\hat{d}^{(2)}$. Since the direction of the fundamental beams is close or coincides with the crystallographic x-axis, the relevant components are d_{33} and $d_{32} = d_{24}$. The unpoled SBN crystal is composed of random needle-like anti-parallel ferroelectric domains which are oriented along z-axis with an average domain size between 2 and 3 μm [11, 12].

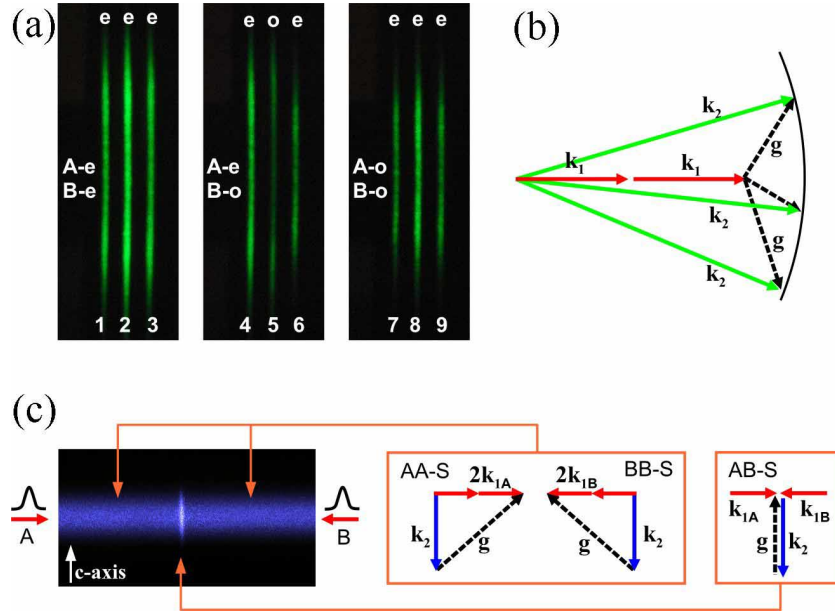


Fig. 2. (a) SH signal (lines) in the QCSH experiment obtained for different polarization orientations of the fundamental beams **A** and **B**. (b) Phase-matching conditions in the QCSH experiment (the case of a single beam); \mathbf{g} being the grating vectors that compensate a phase mismatch in a bulk. (c) Image of the SH signal emitted in the TSH experiment with two counter-propagating fundamental beams **A** and **B**. Trace in the center is a result of mixing of the beams **A** and **B**. In the boxes, it is shown the corresponding phase-matching diagrams of the background single-beam transverse SH scattering **AA-S** and **BB-S** as well as of the transverse SH emission by simultaneous interaction of pulses from **A** and **B**.

In Fig. 2(a) we show the photographs of the forward emitted SH signal observed with intersecting fundamental beams in the QCSH experiment with nanosecond pulses. The three images (left to right) represent the case of (I) two extraordinary polarized fundamental beams, (II) perpendicularly polarized fundamental beams (**A** - extraordinary; **B** - ordinary), and (III) two ordinary polarized fundamental beams. The SH signal is emitted in the form of three well-resolved vertical lines. The side lines (numbered 1, 3, 4, 6, 7, and 9) represent the SH signal emitted separately by each of the fundamental beams. The middle lines (numbered 2, 5, and 8) appear only when both the beams **A** and **B** are present *simultaneously* and hence represent the non-collinear SH generation by two fundamental beams. The polarization state of each SH lines is marked as “e” (extraordinary) or “o” (ordinary). We notice that all but one outputs (line #5) are extraordinary polarized. The presence of this particular ordinary polarized signal defies the previous claims that in SBN crystals only extraordinary SH signal could be generated [13]. This line appears as a result of the parametric process $E_{1A}O_{1B} - O_2$ that is governed by the same component d_{32} also responsible for the process $O_{1A}O_{1B} - E_2$. However, since the phase mismatch for the former interaction is larger, the emitted SH signal is weaker than that in the latter process.

Phase-matching conditions for the SH signals shown in Fig. 2(b) can be represented as

$$\mathbf{k}_{1A} + \mathbf{k}_{1B} + \mathbf{g} = \mathbf{k}_2, \quad (1)$$

where \mathbf{k}_{1A} and \mathbf{k}_{1B} represent the fundamental waves, \mathbf{k}_2 is for the SH wave, and \mathbf{g} is one of the grating vectors supplied by a random structure of the nonlinear quadratic medium. As is seen

Table 1. Interaction types and relevant wave vectors responsible for SHG in the QCSH experiment shown in Figs. 2(a,b); 2γ denotes the intersection angle between the fundamental beams measured inside the sample. The bulk phase mismatches (shown for the forward direction only) are calculated with the refraction index taken from Ref. [14].

SH output	1,4	2	3	5	6,9	7	8
Interaction type	$E_1E_1-E_2$ (AA-S)	$E_1E_1-E_2$ (AB-S)	$E_1E_1-E_2$ (BB-S)	$O_1E_1-O_2$ (AB-S)	$O_1O_1-E_2$ (BB-S)	$O_1O_1-E_2$ (AA-S)	$O_1O_1-E_2$ (AB-S)
k_{1A}	k_{1e}	$k_{1e} \cos \gamma$	k_{1e}	$k_{1e} \cos \gamma$	k_{1o}	k_{1o}	$k_{1e} \cos \gamma$
k_{1B}	k_{1e}	$k_{1e} \cos \gamma$	k_{1e}	$k_{1o} \cos \gamma$	k_{1o}	k_{1o}	$k_{1o} \cos \gamma$
k_2	k_{2e}	k_{2e}	k_{2e}	k_{2o}	k_{2e}	k_{2e}	k_{2e}
$\Delta k [\mu\text{m}^{-1}]$	1.17	1.17	1.17	1.42	0.87	0.87	0.87

from the phase-matching diagram, the vectors \mathbf{g} have different sizes and orientation, but they always lie in the xy -plane. This is in contrast to the SHG with single uniform QPM structures with only a fixed set of the grating vectors available. Due to the randomness of the unpoled SBN crystal, a set of grating vectors with different magnitudes and orientations is available for phase matching. This enables phase matching in an extremely broad range of wavelengths and the SH emission in a broad angular range, as is seen in the images shown in Fig. 2(a). The angular distance between the maxima is of the order of 10 degrees. Moreover, as is demonstrated below, this continuum of grating vectors allows for simultaneous phase matching of several nonlinear parametric processes.

The phase-matching diagram in Fig. 2(b) is valid for all observed processes in the QCSH experiments with nanosecond pulses if we note that \mathbf{k}_{1A} , \mathbf{k}_{1B} , and \mathbf{k}_2 correspond to different wave vectors of the fundamental waves listed in Table 1, where we show only the interactions for which both input beams are purely ordinary or purely extraordinary. For arbitrary polarization of the fundamental beams, the SH signal contains contributions of several processes.

The SH signals recorded in the TSH experiment for the extraordinary polarized counter-propagating beams are shown in Fig. 2(c). This choice of the input polarizations gives the largest intensity of the SH signal. In Fig. 2(c), the horizontal line is given by the SH process originating from each of the beams separately. If both the beams are present, the intensity of this line is just the sum of the intensities of two single-beam SHG process: **AA-S** and **BB-S**. The central bright peak is a result of the **AB-S** interaction in the position where two counter-propagating femtosecond pulses overlap, and it represents the autocorrelation signal of the pulses [9]. In this geometry, the transversely emitted SH wave can only be extraordinary polarized (along the z -axis). Indeed, since the two beams propagate along the x -axis only, two $\chi^{(2)}$ components can be involved in the interactions: $d_{zzz} = d_{33}$ and $d_{zyy} = d_{32}$, so the medium polarization at the doubled frequency can have only z and y components. As the camera “looks” in the y direction, it can only “see” z (extraordinary) polarized signal. Therefore, only signals originating from the processes $E_1E_1 - E_2$ or $O_1O_1 - E_2$ can be observed, as has been confirmed by this experiment. In the insets of Fig. 2(c), the phase-matching conditions for single-beam SH processes (**AA-S** and **BB-S**) and the SH process with counter-propagating fundamental beams (**AB-S**) are shown. The corresponding bulk phase mismatches depend on which particular situation is realized. For a single-beam transverse SHG the phase mismatches are $\Delta k_{oo-e} = \sqrt{k_{2e}^2 + 4k_{1o}^2} = 49.7 \mu\text{m}^{-1}$ and $\Delta k_{ee-e} = \sqrt{k_{2e}^2 + 4k_{1e}^2} = 49.4 \mu\text{m}^{-1}$. For interaction of the counter-propagating fundamental pulses $\Delta k_{oo-e} = \Delta k_{ee-e} = k_{2e} = 36.3 \mu\text{m}^{-1}$.

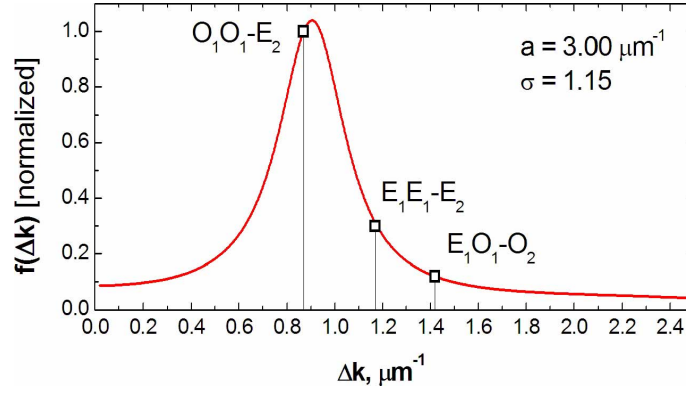


Fig. 3. Function $f(\Delta k)$. Mean size and dispersion of the domains are $a = 3 \mu\text{m}$ and $\sigma = 1.15 \mu\text{m}$, respectively. Squares indicate experimentally determined values of the ratios f_{ee-e}/f_{oo-e} and f_{eo-o}/f_{oo-e} corresponding to $EE - E$, $OO - E$, and $OE - O$ processes.

3. Theoretical model

Earlier studies [3, 6, 15, 16, 17] established that in random nonlinear crystals with anti-parallel domains the SH signal (i) grows linearly with the length of the nonlinear media (unlike the quadratic dependence in perfect structures); (ii) its spectral response characteristic is broader, and it depends on the width of the domain distribution; and (iii) depends on an effective nonlinearity. To discuss these aspects in a quantitative manner, we employ the one-dimensional approach suggested by Le Grand *et al.* [16]. While, strictly speaking, the case considered here is two-dimensional, it turns out that even a simple one-dimensional theory already provides a good agreement with our experimental results. Following Ref. [16], we define the SH intensity in such disordered nonlinear medium as an ensemble average of the SH emission from each individual domain over the domain distribution,

$$I_2^{(o,e)} \propto \frac{2n_{2\omega}}{\epsilon_0 c n_{1\omega}^2} \left(\frac{\omega}{c n_{2\omega}} d_{\text{eff}}^{(o,e)} \right)^2 I_1^2 L, \quad (2)$$

where the effective second-order nonlinearity,

$$d_{\text{eff}} = \mathbf{e}_2 \cdot \hat{d}^{(2)} : \mathbf{e}_{1A} \mathbf{e}_{1B} \sqrt{f(\Delta k, a, \sigma)} \quad (3)$$

depends on the polarizations of the beams **A** and **B** (expressed by unit vectors \mathbf{e}_{1A} and \mathbf{e}_{1B}) and

$$f(\Delta k, a, \sigma) = \frac{4}{\Delta k^2} \frac{1 - \exp(-\sigma^2 \Delta k^2)}{1 + \exp(-\sigma^2 \Delta k^2) + 2 \cos(a \Delta k) \exp(-\sigma^2 \Delta k^2 / 2)} \quad (4)$$

reflects the effect of randomness of nonlinearity on the phase-matching condition, while a and σ denote the mean value and dispersion (standard deviation) of the domain size distribution [16]. This function is shown in Fig. 3. We notice that at large phase mismatch the Eq. (4) has a simple form depending only on Δk ,

$$f(\Delta k, a, \sigma) \propto \frac{1}{\Delta k^2}. \quad (5)$$

For small phase mismatch the maximum of this function, which corresponds to the maximum efficiency of SHG, depends sensitively on the statistical properties of the domain distribution.

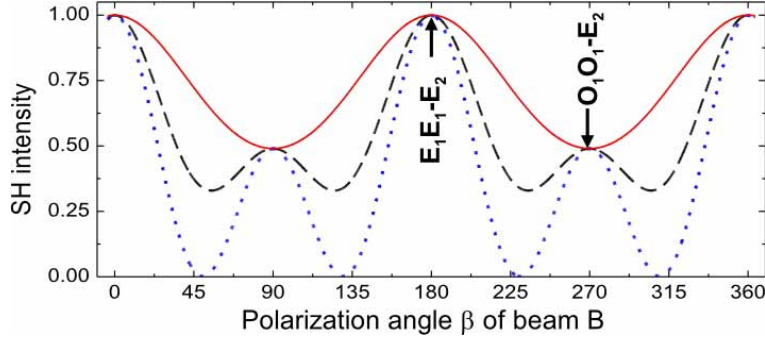


Fig. 4. Theoretically calculated normalized SH intensity as a function of the polarization of the fundamental beam for single beam SHG. Here the extraordinary SH is induced via simultaneously operating $EE - E$ and $OO - E$ processes. Mutually incoherent interaction is shown by dashed line. Mutually coherent interactions depend also on the sign of the ratio of nonlinear coefficients d_{32}/d_{33} shown in solid (dotted) line when this ratio is positive (negative). Two special cases $EE - E$ and $OO - E$ are marked by arrows. $R = 0.48$ is used.

An important consequence of the dependence of effective nonlinearity d_{eff} on the polarization of the interacting beams is the possibility two different processes to contribute simultaneously to the strength of the generated SH signal for a given polarization. For example, an extraordinary polarized SH signal is generated simultaneously by the following two parametric processes: $O_1O_1 - E_2$ and $E_1E_1 - E_2$. On the other hand, an ordinary SH signal builds up from contributions created via $E_{1A}O_{1B} - O_2$ and $O_{1A}E_{1B} - O_2$ interactions. Had these processes been taking place in the perfect QPM structures they would naturally have contributed coherently to the total SH signal. In fact, this has been demonstrated in the recent experiment with a QPM grating in LiNbO₃ crystal that supported simultaneously $E_1E_1 - E_2$ and $O_1O_1 - E_2$ interactions [10]. In that case a strong interference between two simultaneously generated SH waves has been observed. However, here we may expect that the mutual coherence between various SH contributions may be affected by the randomness of the QPM structure. This will be immediately reflected in the strength of an effective nonlinearity and, consequently, the intensity of the SH output. For instance, for extraordinary SH waves the effective nonlinearity is

$$\begin{aligned} |d_{\text{eff}}^{(e)}|^2 &= d_{33}^2 f(\Delta k_{ee-e}) \cos^4 \beta + d_{32}^2 f(\Delta k_{oo-e}) \sin^4 \beta \\ &= d_{33}^2 f(\Delta k_{ee-e}) (\cos^4 \beta + R \sin^4 \beta), \end{aligned} \quad (6)$$

in the incoherent case, and

$$\begin{aligned} |d_{\text{eff}}^{(e)}|^2 &= \left(d_{33} \sqrt{f(\Delta k_{ee-e})} \cos^2 \beta + d_{32} \sqrt{f(\Delta k_{oo-e})} \right)^2 \\ &= d_{33}^2 f(\Delta k_{ee-e}) \left(\cos^2 \beta \pm \sqrt{R} \sin^2 \beta \right)^2, \end{aligned} \quad (7)$$

if both SH contributions are mutually coherent. The parameter R is defined as

$$R = \frac{f(\Delta k_{oo-e})}{f(\Delta k_{ee-e})} \left(\frac{d_{32}}{d_{33}} \right)^2, \quad (8)$$

and the \pm sign in Eq. (7) depends on a relative sign of d_{32} and d_{33} .

Table 2 shows all possible forms of the nonlinear coefficients corresponding to the fundamental nonlinear processes relevant to our experiments. In order to demonstrate the effect of

the simultaneous operation of two different parametric processes in SHG, in Fig. 4 we plot the intensity of the extraordinary polarized SH signal calculated theoretically (in arbitrary units) as a function of the input polarization of the beam **B** (expressed by its azimuthal angle β). The polarization angle is measured counterclockwise from zero which corresponds to the extraordinary polarization. Since, in general, the extraordinary SH signal consists of two contributions, $EE - E$ and $OO - E$, the intensity of the SH signal will depend on whether contributions from both of these processes add coherently or not. It also appears that in the former case the total generated signal depends on the sign of the ratio of the nonlinear coefficients d_{33}/d_{32} . Interestingly enough, there is no data available in the literature regarding the signs of those two nonlinear components of the $\chi^{(2)}$ tensor. Therefore, the plots in Fig. 4(a) describe all possible scenarios. The dashed line refers to the mutually incoherent contributions. The solid and dotted plots represent the mutually coherent case but differ in sign of d_{32}/d_{33} (positive in the former and negative in the latter cases). It is clear that the character of those plots change significantly depending on whether contributions from different processes add coherently or incoherently. In particular, for the mutually coherent processes and opposite signs of nonlinear coefficients the SH signal vanishes for a particular polarization of the input beam. This behavior is analogous to the one reported recently in the case of the QPM grating in lithium niobate [10].

4. Results and discussion

Experimentally measured dependence of the SH intensity vs. the input polarization of the fundamental beams is shown in Figs. 5(a-d). In all these plots, the polarization of beam **B** is varied (via its azimuthal angle β) while the polarization of the beam **A** is set to one of the following three states: extraordinary, $\alpha = 0$ (filled squares); mixed, $0^\circ < \alpha < 90^\circ$ (open circles), and ordinary, $\alpha = 90^\circ$ (open squares). Figures 5(a-b) and 5(c-d) show the results of both QCSH and TSH experiments, respectively. The lines show the theoretical results in the absence of interference between different contributions to the SH signal. We compare, e.g., the data shown in Fig. 5(a) by filled circles with the data shown in Fig. 4 by a dashed line, which depicts the SH signal emitted by a single beam. We note a very good agreement between theory and experiment; this confirms that disorder in the domain distribution in our crystal causes simultaneous processes to contribute incoherently into the overall signal.

The use of two-beam SHG with weak noncollinearity in the QCSH experiment is crucial for the observation of SH scattering with pure ordinary polarization. We believe the experiment presented here is the first experiment that shows that such process is indeed possible in the SBN crystal [see Fig. 5(b)]. This happens when the two fundamental beams are orthogonally polarized (ordinary and extraordinary). Then SH is emitted via either $E_{1A}O_{1B} - O_2$ or $O_{1A}E_{1B} - O_2$ interaction. Ordinary SH can also be observed with a single beam SH generation. The signal reaches its maximum when the input polarization is at 45° with respect to the YZ axes, and vanishes for ordinary or extraordinary polarization [see Fig. 5(b)]. From the definition of the

Table 2. Effective nonlinear coefficients for separate SHG processes in SBN crystals.

SH with	single beam A	single beam B	two beams A and B	Relevant experiment
d_{ee-e}	$d_{33} \cos^2 \alpha$	$d_{33} \cos^2 \beta$	$2d_{33} \cos \alpha \cos \beta$	TSH, QCSH
d_{oo-e}	$d_{32} \sin^2 \alpha$	$d_{32} \sin^2 \beta$	$2d_{32} \sin \alpha \sin \beta$	TSH, QCSH
d_{oe-o}	$2d_{32} \sin \alpha \cos \alpha$	$2d_{32} \sin \beta \cos \beta$	$2d_{32} \sin \alpha \cos \beta$	QCSH
d_{eo-o}	$2d_{32} \sin \alpha \cos \alpha$	$2d_{32} \sin \beta \cos \beta$	$2d_{32} \cos \alpha \sin \beta$	QCSH

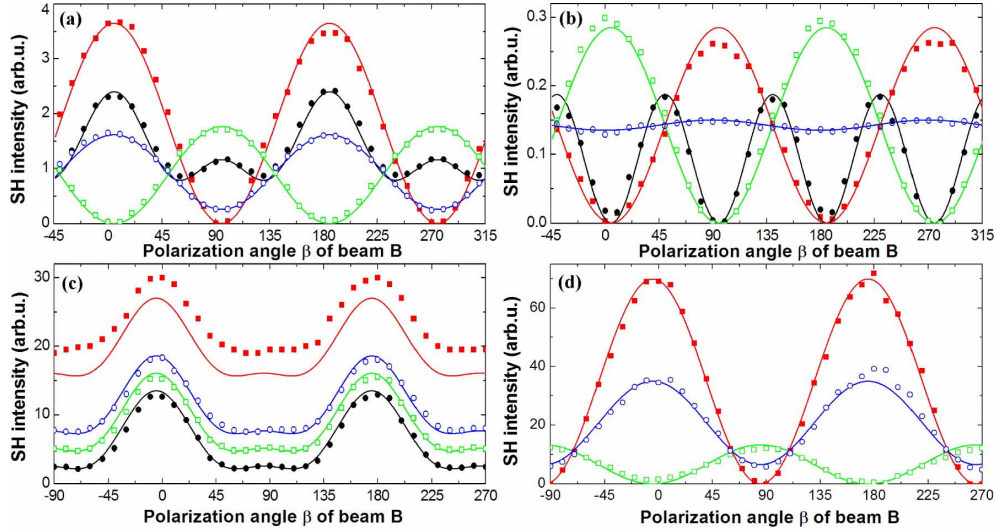


Fig. 5. Experimentally observed SH signal vs. input polarization angle β for three fixed polarizations of beam **A**: extraordinary - red full squares; mixed - blue open circles, and ordinary - green open squares. Single beam SH (black full circle); Lines show theoretical results. (a) extraordinary SH; (b) ordinary SH; both (a) and (b) are for SHG in the QCSH experiment. (c) Background TSH and single beam TSH; (d) TSH emission via **A** and **B** pulse mixing. Mixed polarizations: $\alpha = 30^\circ, 43.5^\circ, 45^\circ, 45^\circ$ for a,b,c,d plot respectively.

parameter R in Eq. (8) we obtain

$$R = \frac{f(\Delta k_{oo-e})}{f(\Delta k_{ee-e})} \left(\frac{d_{32}}{d_{33}} \right)^2 = \frac{I_{oo-e}}{I_{ee-e}}, \quad (9)$$

where I_{ee-e} is the SH signal at $\beta = 0^\circ (180^\circ)$, and I_{oo-e} is the SH signal at $\beta = 90^\circ (270^\circ)$ for the experiments with a single beam [see Fig. 5(a) and Fig. 5(c)]. Therefore, one can directly find the value of R as a ratio of the intensities of the SH signal taken in two different polarization arrangements. In the QCSH experiment, the best theoretical fit is obtained for $R = 0.48$ [Fig. 5(a,b)], while in the case of TSH experiment the best fit is obtained for $R = 0.19$ [Fig. 5(c,d)]. The value $R = 0.48$ is also used in our theoretical plots in Fig. 4. As we pointed out above, for the TSH experiment with counter-propagating fundamentals $\Delta k_{oo-e} \sim \Delta k_{ee-e}$ and, consequently, $f(\Delta k_{oo-e})/f(\Delta k_{ee-e}) \approx 1$. Subsequently, we obtain $|d_{32}/d_{33}| = 0.44$. This is close to the value of 0.5 obtained in Ref. [13] and the theoretical value of 0.39 given in Ref. [18]. After having found $|d_{32}/d_{33}|$, one can estimate the mean value a and dispersion σ of the domain distribution. To this end we measure the intensity of the emitted SH in the central part of the emission lines #5 ($OE - O$ process), #8 ($OO - E$ process) and #2 ($EE - E$ process) seen in Fig. 2. From these measurements, we evaluate the ratios: $f(\Delta k_{oe-o})/f(\Delta k_{oo-e}) = 0.12$ and $f(\Delta k_{ee-e})/f(\Delta k_{oo-e}) = 0.3$, and then from Eq. (4) we find $a = 3.25 \mu\text{m}$ and $\sigma = 1.15 \mu\text{m}$. These values are consistent with Refs. [11, 12] and are used to calculate the curve in Fig. 3.

5. Conclusions

We have studied the second-harmonic generation in unpoled quadratic nonlinear crystals with disordered ferroelectric domains. We have demonstrated that such crystals enable the realization of several different parametric processes including collinear, non-collinear and transverse

second-harmonic generation. In most of the cases, these parametric processes occur simultaneously, contributing incoherently to the overall strength of the second-harmonic signal. We have analyzed the polarization properties of the parametric processes and employed them to determine the relative strength of two relevant components of the second-order susceptibility tensor, such as the ratio d_{32}/d_{33} . We have demonstrated that, by measuring the power of the second harmonics in a few different processes, we can determine the statistical properties of the disordered domain distribution such as an average size of the domains and their dispersion.

Acknowledgments

The authors from Universitat Politècnica de Catalunya thank the project FIS2005-07931-C03-03. The Australian researchers acknowledge support by the Australian Research Council. Solomon Saltiel thanks the Australian National University and Universitat Politècnica de Catalunya for hospitality and support.